

Electronic Supplementary Information

Single-molecule force-unfolding of titin I27 reveals correlation between size of surrounding anions and its mechanical stability

Mohd Muddassir,^a Bharat Manna,^b Priyanka Singh,^a Surjeet Singh,^a Rajesh Kumar,^c Amit Ghosh^b and Deepak Sharma ^{*a}

^a*Council of Scientific and Industrial Research–Institute of Microbial Technology, Sector 39A, Chandigarh, India*

^b*School of Energy Science and Engineering, Indian Institute of Technology Kharagpur, Kharagpur, India*

^c*School of Basic and Applied Sciences, Central University of Punjab, Bathinda, India*

***Corresponding author:** E-mail: deepaks@imtech.res.in, CSIR-Institute of Microbial Technology, Sector 39A, Chandigarh, India.

**Email- deepaks@imtech.res.in*

Table of Content

- (1) Experimental Methods.
- (2) Table S1- Physico-chemical parameters of different anions.
- (3) Table S2 – Results from equilibrium chemical denaturation studies.
- (4) Table S3- SMD simulation results for different pulling velocities.
- (5) Figure S1- Schematic of the Single-molecule pulling Experiment
- (6) Figure S2- Contour length changes (ΔL_C) of (I27)₈ in the absence or presence of different anions.
- (7) Figure S3-The representative force–extension curves of (I27)₈ in absence and presence of different anions.
- (8) Figure S4 – The in situ study to monitor modulation of mechanical stability upon changing anions.
- (9) Figure S5- Loading-rate dependent experiment
- (10) Figure S6 - Equilibrium chemical denaturation of I27.
- (11) Figure S7- Mechanical unfolding energy landscapes.
- (12) Figure S8 - Comparison of I27 structure obtained from SMD simulations before and after the main burst phase.

Experimental Methods

The plasmid and reagents: The plasmid (pQE80L-(I27)₈) encoding (I27)₈ was a kind gift from Prof. S.R.K. Ainavarapu. The plasmid encoding His tagged I27 module (I27 with 4 Gly residues at N-terminus and 6 amino acid tag (LPETGSS) at the C-terminus of the protein henceforth referred as I27-M) was a kind gift from Dr. Sabyasachi Rakshit. The salts were all purchased from Sigma-Aldrich as analytical reagents with purity >99%.

Protein expression and purification: Recombinant His-(I27)₈ was overexpressed in *Escherichia coli* strain Rosetta2(DE3) (Invitrogen). The cells were grown at 37°C until optical density at 600nm (OD₆₀₀) reached 0.5–0.6. The protein expression was induced with 0.3 mM isopropyl-β-D-thiogalactoside (IPTG) at 37°C for 3 hours. The cells were harvested and lysed with lysis buffer (20mM HEPES, 150mMNaCl, protease inhibitor cocktail, and phenylmethylsulfonyl fluoride [PMSF]) using lysozyme, followed by sonication. The lysate was centrifuged at 10000×g for 45 min, and protein was purified from the supernatant using HisPur cobalt resin (Thermo cat.#89965). His-(I27)₈ was eluted with 300mM imidazole and dialyzed in PB. To improve purity, the protein was next subjected to size exclusion chromatography (HiLoad 16/600 Superdex 200pg, GE healthcare).

The His-I27-M was purified using procedure described above for (I27)₈. The His₆ tag was further cleaved by overnight incubation of the purified protein with His₆-TEV (molar ratio, His-I27-M/His₆-TEV:20/1) protease at 4°C. The His₆-TEV was removed from solution using

cobalt metal affinity column to obtain purified I27-M. The purity of the protein was confirmed using sodium dodecyl sulphate polyacrylamide gel electrophoresis (SDS-PAGE) analysis.

Mechanical unfolding: All SMFS experiments were carried out with a commercial atomic force microscope (Force Robot 00574, JPK Instruments). The force–distance curves were constructed in commercial software from JPK and analyzed by custom-written procedures in Igor pro 6.2 (Wavemetrics, Inc.).

The glass coverslips (Fisher Scientific) for holding a protein sample were cleaned by heating with chromium acid solution followed by extensive washing with Milli-Q water. All AFM force measurements were carried out at 25°C and at pH 7.4. For single-protein pulling experiments, 50 μL of a (I27)₈ protein solution (~100–200 $\mu\text{g}/\text{ml}$) was added, and the protein was allowed to adsorb onto the coverslip for ~15 min before the pulling experiments. After that, the fluid chamber was filled with PB (800 μL) with or without desired salt. The AFM experiments were conducted after allowing the system to equilibrate for 30 min.

The cantilever tip was next brought into contact with the glass coverslip to pick up the polyprotein. The presence of tandem repeats amplifies the number of force events per extension of the polyprotein and enhances the signal-to-noise ratio. The force extension curves were fitted to worm-like chain model using persistence length (p) of 0.4nm to obtain force ($F(x)$) at extension x :

$$F(x) = \frac{k_B T}{P} \left(\frac{1}{4(1-x/L)^2} - \frac{1}{4} + \frac{x}{L} \right)$$

Where p is the persistence length, and L is the total contour length of the protein, K_B is Boltzmann constant and T is absolute temperature ¹.

The contour length increment is a measure of the number of amino acid residues released upon complete extension of the protein. Ig domain I27 consists of 89 amino acid residues, and in the folded state, N- and C-terminal residues are separated by ~4.3 nm. Thus, the force-induced extension of I27 to the fully stretched unfolded state should show a contour length increment (ΔL_c) of ~28 nm ($89 \times 0.36 \text{ nm} - 4.3 \text{ nm} = 27.7 \text{ nm}$). The average unfolding force was obtained by fitting the force histogram to a Gaussian distribution.

The spring constant of each individual cantilever tip (Si_3N_4 , APP NANO) was calibrated in solution by the thermal fluctuation method and was found to be in the range of 42–75 $\text{mN}\cdot\text{m}^{-1}$. To obtain kinetic parameters, the polyprotein was stretched at varying pulling speed from 100 to 6400 nm/sec . The unfolding rate constant α_0 at zero force and the distance between the folded state and the transition state Δx_u were estimated by means of the Bell–Evans model according to published procedures²⁻⁴.

Equilibrium denaturation: The presence of additional residues mentioned above in I27-M has no significant impact on structural stability of wt I27 as evident by Far-UV circular dichroism (CD) (Figure S5) spectra and unfolding free energy in PB which is similar to as reported before⁵. The equilibrium denaturation experiments were carried out with I27-M. The Urea was used as denaturant. The protein (20 μM) was incubated with increasing concentration of Urea from 0 M to 9.0 M Urea at 25°C for 6h. The denaturation was monitored by loss of secondary structure using CD at 229nm, and intensity of tryptophan fluorescence at 313nm upon excitation at 280nm. The data was fitted to a two state transition using equation:

$$Y_{obs} = \frac{(C_N + M_N[D]) + (C_U + M_U[D]) \exp\left[\frac{-\Delta G_D + m_g[D]}{RT}\right]}{1 + \exp\left[\frac{-\Delta G_D + m_g[D]}{RT}\right]}$$

Y_{obs} parameter represents the observed signal, and C_N , C_U , and M_N , M_U represent intercepts and slopes of native (C_N , M_N) and unfolded (C_U , M_U) baselines, respectively, $[D]$ is the concentration of urea in M, R is the gas constant, ΔG_D , the free energy associated with the transition, and m_g , the surface area of the protein exposed by the solvent. C_m , the transition mid-point of urea concentration, was calculated as $C_m = \Delta G_D/m_g$.

SMD simulation: The initial structure for the molecular dynamics (MD) simulation of the Ig-like domain (I27) from titin I-band was obtained from Protein Data Bank entry 1TIT⁶. The protein was solvated in an explicit aqueous solvent using the TIP3⁷ water model with a periodic boundary condition. The water box was first neutralized, followed by addition of 1.0 M NaCl in one system and 1.0 M NaI in another for comparing the unfolding behavior of I27. Minimization was performed in the NPT ensemble with a distance cutoff of 12.0 Å for nonbonded interactions. The particle-mesh Ewald method⁸ was employed to analyze long-range electrostatic interactions. Equilibration was performed for 1.0ns at a constant temperature of 300 K using Langevin dynamics, and pressure was maintained at 1.0atm with a Nosé-Hoover Langevin piston^{9, 10}. The equations of motion were integrated with a time step of 2.0fs. SMD simulation was carried out at constant velocity (SMD-CV protocol) for a total stretching of 100Å¹¹. The SMD production run was performed for 200ps with constant velocity of 0.5Å/ps and for 1.0ns at a comparatively lower pulling velocity of 0.1Å/ps, respectively. All the systems were prepared in VMD¹², and SMD simulations were performed by means of the NAMD¹³ molecular dynamics package using CHARMM36 force field¹⁴.

Table S1.- Physico-chemical parameters of different anions.

Anions	Thermochemical Radii (Å) ^{15, 16}		Ionic Polarizability (Å ³) ¹⁷	Molar Surface Tension Increment (mN.L/m.M) ¹⁸	Lyotropic number ¹⁸	Free energy of hydration ΔG_{hyd} (kJ/mol) ¹⁸	Dipole moment (D) ¹⁹	Mechanical Stability (pN)
	<i>Ref 15</i>	<i>Ref 16</i>						
Cl ⁻	1.81	1.68	3.73	1.63	10	340	8.97	174
Br ⁻	1.96	1.90	5.07	1.31	11.3	315	9.09	153
NO ₃ ⁻	2.02	2.0	4.48	1.18	11.6	300	15.07	151
I ⁻	2.20	2.11	7.16	1.02	12.5	275	9.2	145
ClO ₄ ⁻	2.22	2.25	5.26	1.4	11.8	430	-	144
SO ₄ ²⁻	2.31	2.30	6.33	2.74	2.0	1080	-	138

Table S2. Far-UV CD (229 nm) and tryptophan fluorescence (excitation.280 nm; emission 313 nm) monitored urea-induced unfolding free energy (ΔG_D), surface area exposed by the solvent (m_g) and urea-unfolding midpoint (C_m) for I27 at pH 7.4, 25 °C.

[Salt]	CD			Fluorescence		
	ΔG_D	m_g	C_m	ΔG_D	m_g	C_m
Control (PB)	7.4	1.4	5.3	7.1	1.3	5.5
0.2 M NaBr	6.6	1.3	5.1	5.5	1.1	5.0
1.0 M NaClO ₄	5.1	1.3	3.9	4.9	1.2	4.1

* ΔG_D , m_g and C_m are reported in kcal mol⁻¹, kcal mol⁻¹ M⁻¹, and M, respectively. The uncertainty in the values of ΔG_D and m_g are ± 0.5 kcal mol⁻¹, ± 0.2 kcal mol⁻¹M⁻¹, respectively.

Table S3. SMD simulation results at different pulling velocities.

Expt. No.	Pulling Position	Solvent System						Pulling Velocity (Å/ps)
		1M NaCl		1M NaI		Water		
		Peak at Extension (Å)	Force at Peak (pN)	Peak at Extension (Å)	Force at Peak (pN)	Peak at Extension (Å)	Force at Peak (pN)	
1	N-Termini	21.64	3473.28	21.07	3331.52	20.67	3162.55	0.5
2	N-Termini	21.24	3051.29	19.19	2891.21	16.20	2955.09	0.5
3	N-Termini	22.01	3536.29	20.39	3394.19	19.42	3121.20	0.5
4	C-Termini	14.60	3190.91	15.19	3055.28	-	-	0.5
5	C-Termini	13.72	3066.88	15.07	2915.15	-	-	0.5
6	C-Termini	15.74	3175.68	15.08	3017.79	-	-	0.5
7	N-Termini	18.22	2157.60	15.00	2012.98	-	-	0.1
8	C-Termini	13.32	2093.12	13.13	1995.58	-	-	0.1

Figure S1: Schematic of Single-molecule pulling experiment. A schematic of the sequence of events during single-molecule pulling experiments using atomic force spectroscopy. The protein is deposited on a glass surface. The cantilever tip picks up a polyprotein molecule. Retraction of the piezoelectric positioner stretches the protein which in turn applies a restoring force on the protein. At a certain force, one of the domains unfolds resulting in relaxation of the cantilever to its original position. Further stretching leads to sequential unfolding of remaining domains held between the cantilever and glass surface. Orange color spots represent ions present in surrounding medium.

Figure S2: Contour length changes (ΔL_C) of (I27)₈ in the absence or presence of different anions.

Figure S3: The representative force–extension curves of (I27)₈ in absence and presence of different anions. Red lines correspond to wormlike chain (WLC) fit.

Figure S4: The in situ study to monitor modulation of mechanical stability upon changing anions. The mechanical stability of the protein was measured in the presence of 1M NaCl (top panel). The buffer was then replaced in situ with that containing 1M NaClO₄ in place of NaCl and unfolding force was monitored (middle panel). The buffer was further replaced back to 1M NaCl (Lower Panel). All experiments were conducted with the same cantilever at a pulling speed of 400 nm·s⁻¹. The Gaussian fit of the force histogram is presented as a solid red curve.

Figure S5: Loading-rate dependent experiment. Loading-rate dependence of the unfolding force of (I27)₈ in PB (A) in the absence (■) or presence (●) of 0.2 M NaBr (B) or (▲) 1M NaClO₄ (C). The single polyprotein molecule was stretched at different pulling speeds. The symbols correspond to the average of the force obtained at a single pulling speed, and the experimental data were fitted to the Bell–Evans model.

Figure S6: Equilibrium chemical denaturation of I27-M. Panels (A) and (B) show far-UV CD and tryptophan fluorescence spectra of I27-M, respectively, in the absence (black curve) and presence (pink curve) of 8.4 M urea at pH 7.4, 25 °C. Panels (C) and (D) show the far-UV CD (229 nm) and tryptophan fluorescence (ex: 280, em: 313 nm) monitored urea-induced unfolding profiles of I27, respectively, in the phosphate buffer only (black symbols), with 0.2 M NaBr (yellow symbols) and 1.0 M NaClO₄ (blue symbols) at pH 7.4, 25 °C. Panels (E) and (F) show the far-UV CD (229 nm) and tryptophan fluorescence (ex: 280, em: 313 nm) monitored normalized urea-induced unfolding profiles of I27-M, respectively, in the phosphate buffer only (black curve), with 0.2 M NaBr (yellow curve) and 1.0 M NaClO₄ (blue curve) at pH 7.4, 25 °C. The solid lines in panels (E) and (F) represent nonlinear least-squares fit using the standard two-state equation²⁰.

Figure S7: Mechanical unfolding energy landscapes of I27 (black) in PB alone (A) and I27 in the presence of PB with 0.2 M NaBr (light yellow) (B) or 1M NaClO₄ (Blue) (C). N,

native state; T, transition state; and U, unfolded state.

Figure S8: Comparison of I27 structure obtained from SMD simulations before and after the main burst phase. Structure of I27 in a NaCl or NaI (A and C) solvated system, respectively, when all the hydrogen bonds between strands A and B and between strands A' and G are intact. After the main burst phase with all the interstrand hydrogen bonds broken between strands A and B and between strands A' and G in the presence of NaCl or NaI (B and D), respectively. Snapshots were taken at the extension of ~ 5 Å (A,C) and ~ 20 Å (B,D), respectively.

Figure S1

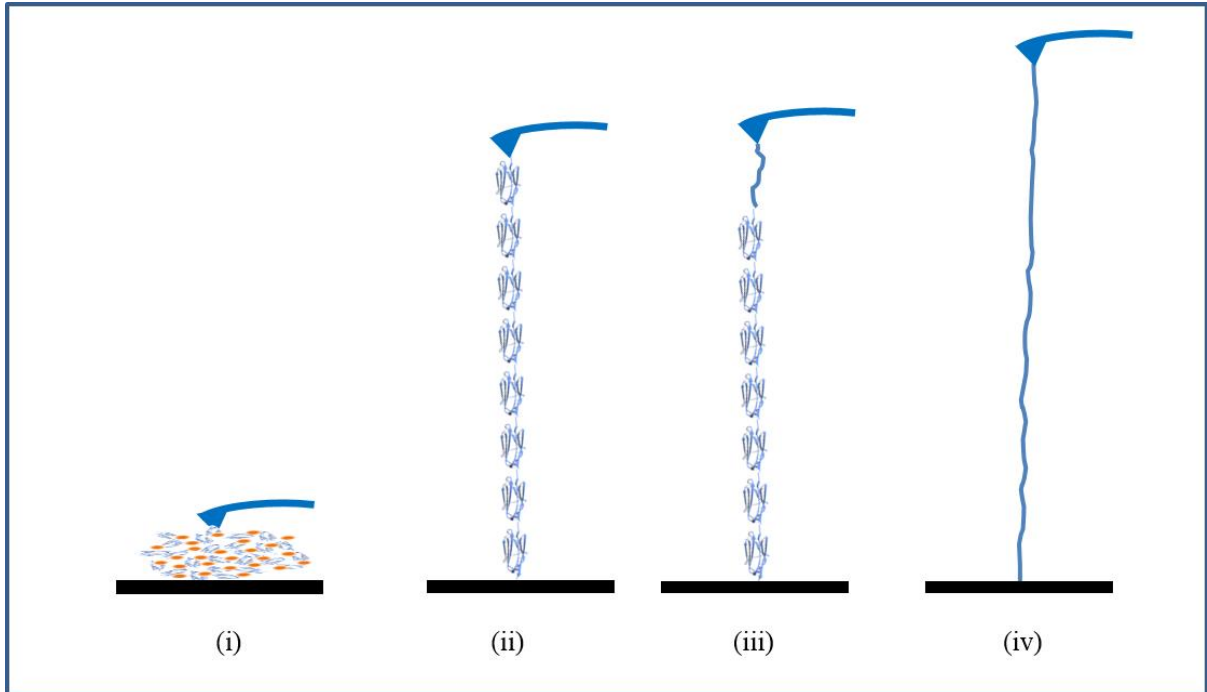


Figure S2

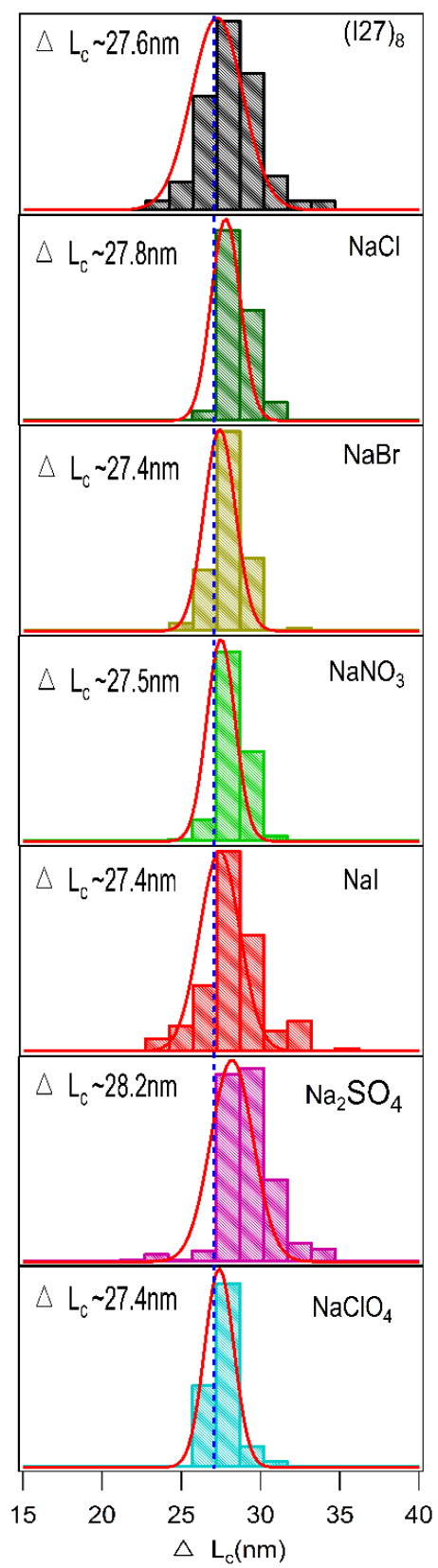


Figure S3

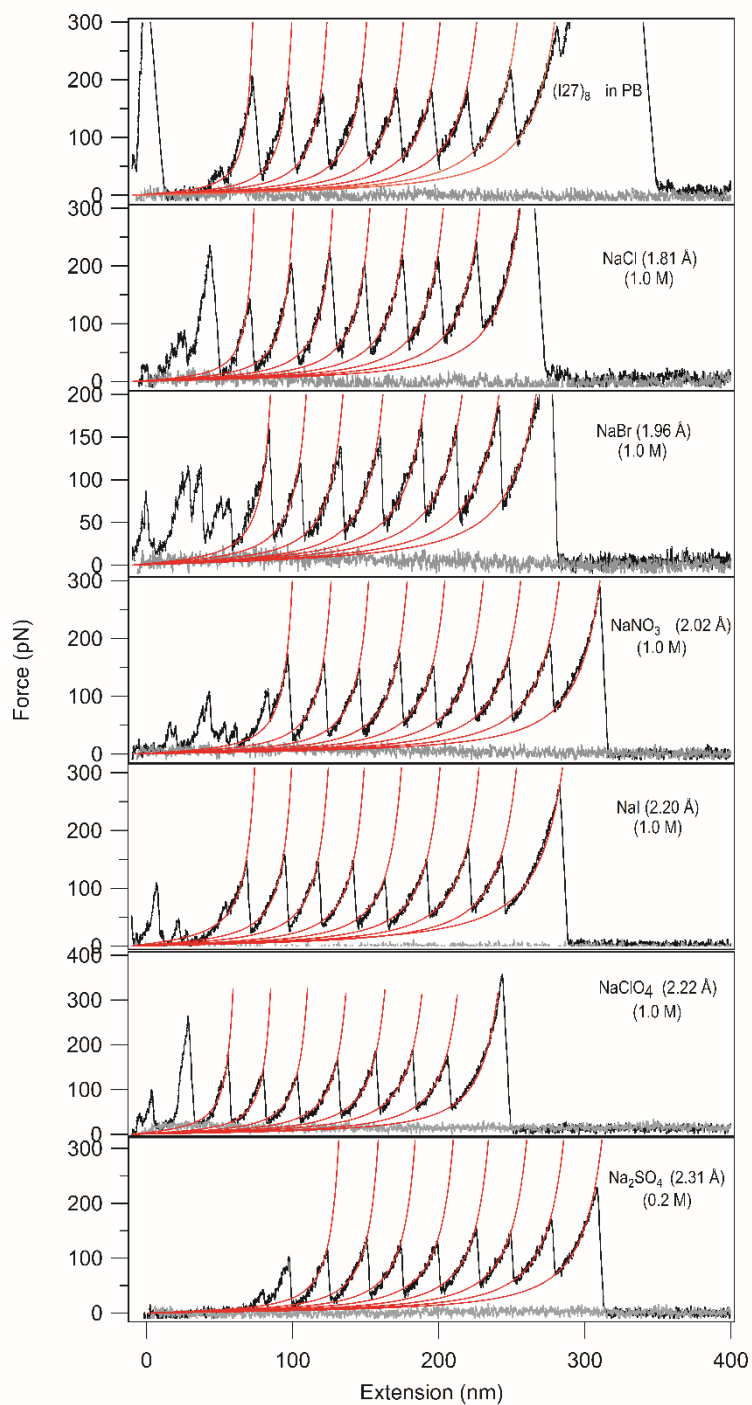


Figure S4

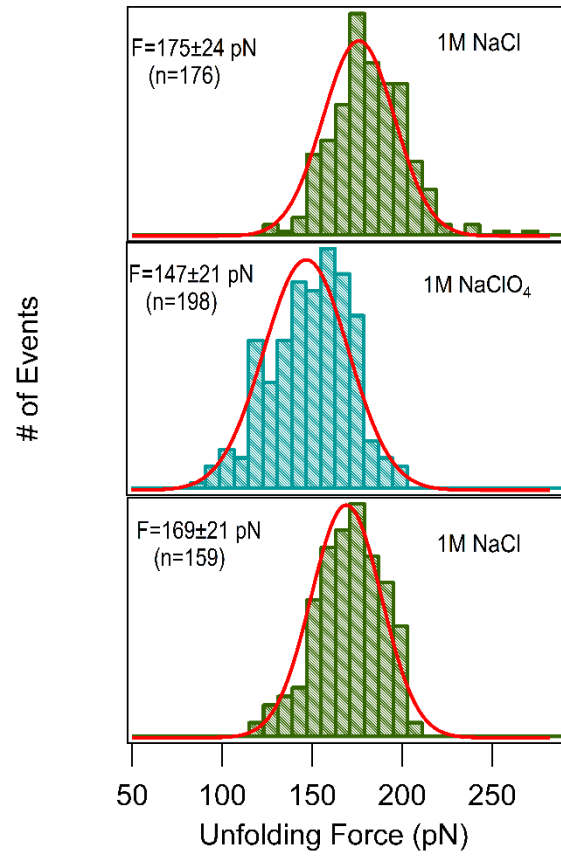


Figure S5

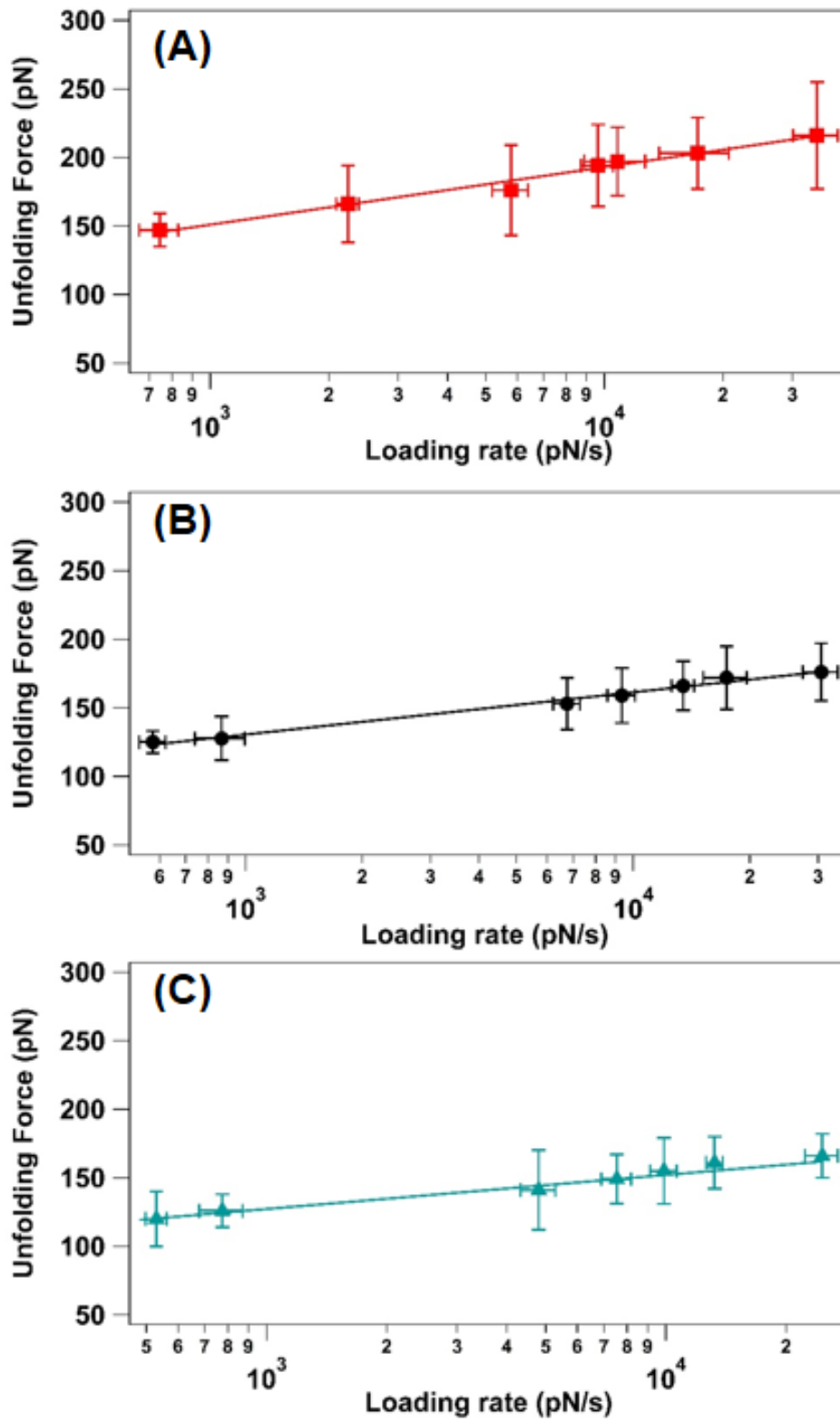


Figure S6

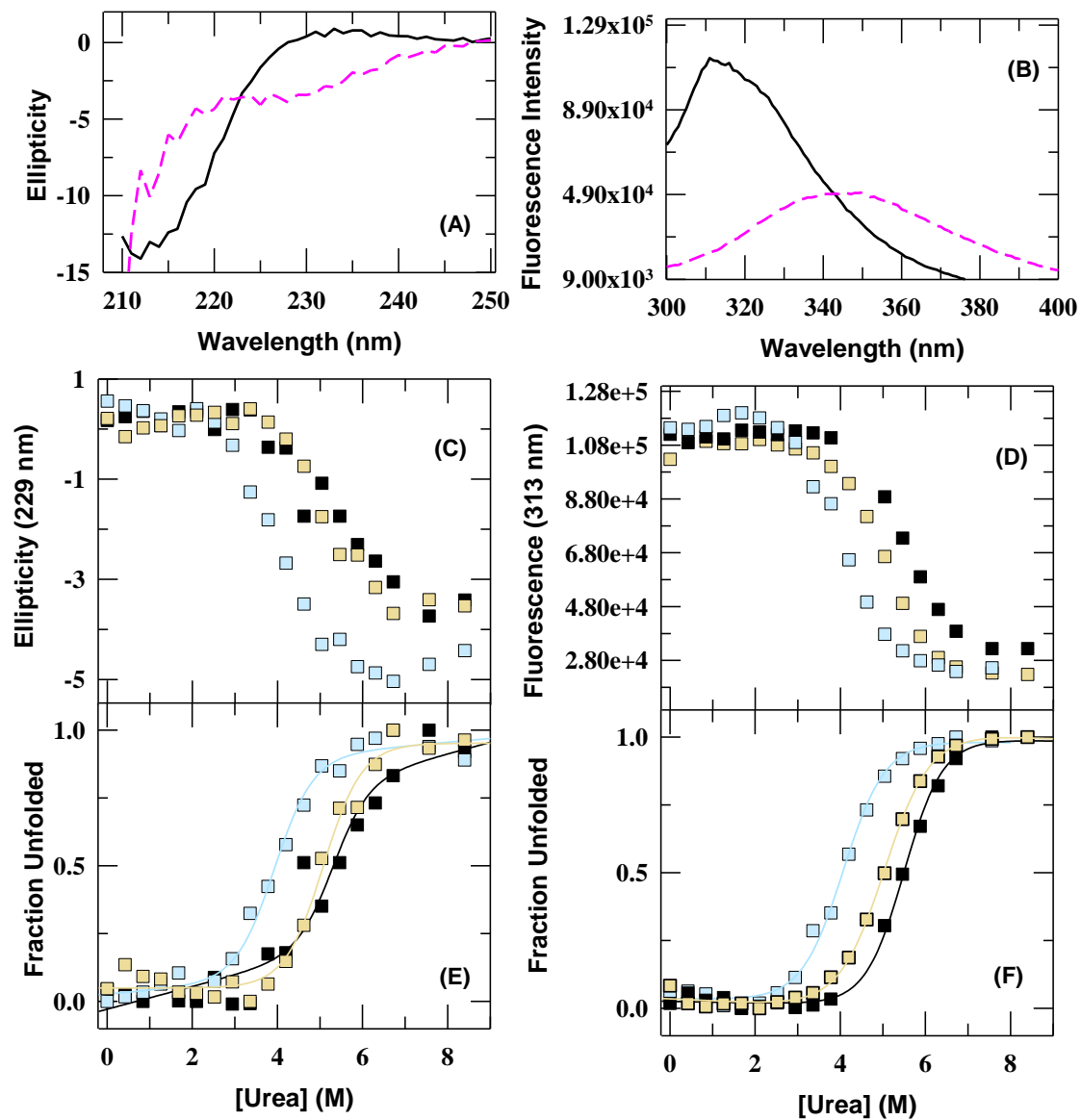


Figure S7

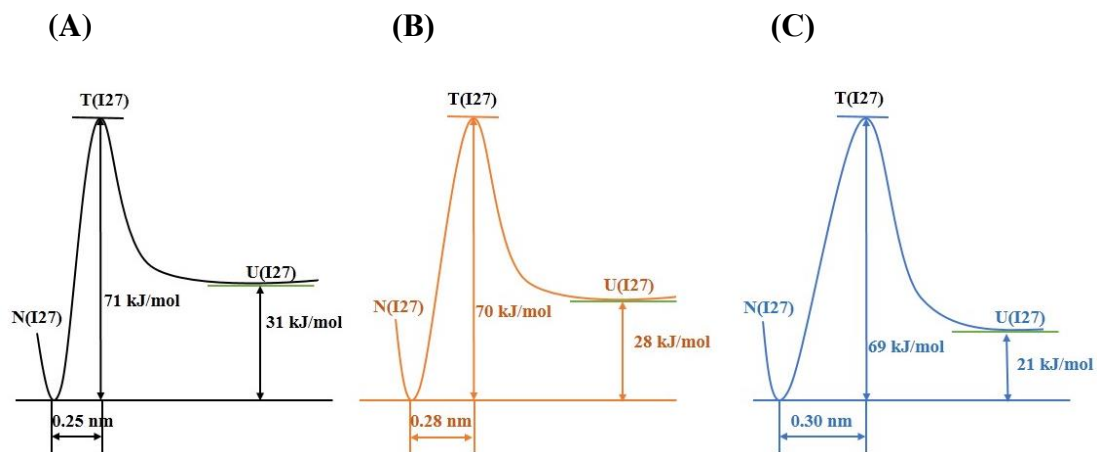
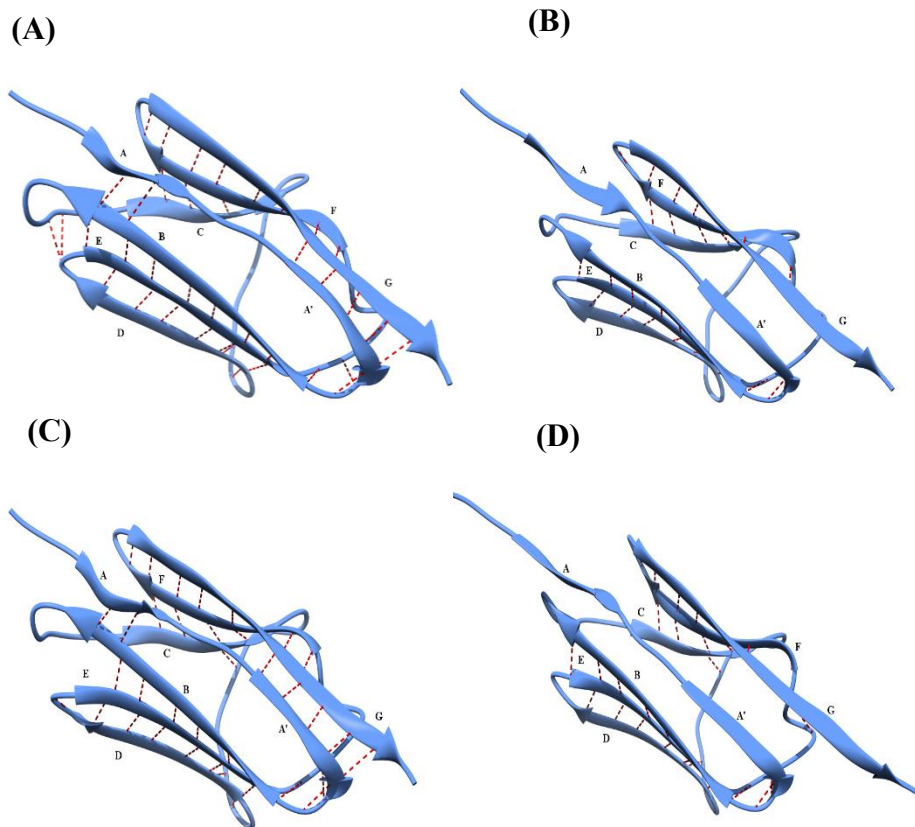


Figure S8



References

1. J. F. Marko and E. D. Siggia, *Macromolecules*, 1995, **28**, 8759-8770.
2. G. I. Bell, *Science*, 1978, **200**, 618-627.
3. E. Evans and K. Ritchie, *Biophys J*, 1997, **72**, 1541-1555.
4. D. L. Guzmán, A. Randall, P. Baldi and Z. Guan, *Proceedings of the National Academy of Sciences*, 2010, **107**, 1989-1994.
5. J. Oroz, M. Bruix, D. V. Laurents, A. Galera-Prat, J. Schonfelder, F. J. Canada and M. Carrion-Vazquez, *Structure*, 2016, **24**, 606-616.
6. S. Improta, A. S. Politou and A. Pastore, *Structure*, 1996, **4**, 323-337.
7. W. L. Jorgensen, J. Chandrasekhar, J. D. Madura, R. W. Impey and M. L. Klein, *The Journal of Chemical Physics*, 1983, **79**, 926-935.
8. T. Darden, D. York and L. Pedersen, *The Journal of Chemical Physics*, 1993, **98**, 10089-10092.
9. S. E. Feller, Y. Zhang, R. W. Pastor and B. R. Brooks, *The Journal of Chemical Physics*, 1995, **103**, 4613-4621.
10. G. J. Martyna, D. J. Tobias and M. L. Klein, *The Journal of Chemical Physics*, 1994, **101**, 4177-4189.
11. S. Izrailev, S. Stepaniants, M. Balsera, Y. Oono and K. Schulten, *Biophysical Journal*, 1997, **72**, 1568-1581.
12. W. Humphrey, A. Dalke and K. Schulten, *Journal of Molecular Graphics*, 1996, **14**, 33-38.
13. J. C. Phillips, R. Braun, W. Wang, J. Gumbart, E. Tajkhorshid, E. Villa, C. Chipot, R. D. Skeel, L. Kalé and K. Schulten, *Journal of Computational Chemistry*, 2005, **26**, 1781-1802.
14. R. B. Best, X. Zhu, J. Shim, P. E. M. Lopes, J. Mittal, M. Feig and A. D. MacKerell, *Journal of Chemical Theory and Computation*, 2012, **8**, 3257-3273.
15. M. C. Simoes, K. J. Hughes, D. B. Ingham, L. Ma and M. Pourkashanian, *Inorganic Chemistry*, 2017, **56**, 7566-7573.
16. H. K. Roobottom, H. D. B. Jenkins, J. Passmore and L. Glasser, *Journal of Chemical Education*, 1999, **76**, 1570.
17. F. W. Tavares, D. Bratko, H. W. Blanch and J. M. Prausnitz, *The Journal of Physical Chemistry B*, 2004, **108**, 9228-9235.
18. P. Lo Nostro, B. W. Ninham, S. Milani, A. Lo Nostro, G. Pesavento and P. Baglioni, *Biophysical Chemistry*, 2006, **124**, 208-213.
19. S. Mondal, S. Roy, S. Ghosh, K. Mahali and B. K. Dolui, *Journal of Solution Chemistry*, 2016, **45**, 1755-1772.
20. M. M. Santoro and D. W. Bolen, *Biochemistry*, 1988, **27**, 8063-8068.